CHAPTER 3

RESULTS AND DISCUSSION

The determination of Cu, Cd and Pb in rainwater samples were carried out by GFAAS after preconcentration by Amberlite IRC-748 resin.

3.1 Optimization of graphite furnace atomic absorption spectrometer (GFAAS)

3.1.1 Pyrolysis temperature

The purpose of the thermal pyrolysis step is to remove as much of the matrix as possible prior to atomization. This decreases the possibility of chemical interference and reduces the magnitude of the background signal (AAnalyst 800, Perkin-Elmer). The results are shown in Table 3-1 to 3-3 and Figure 3-1 to 3-3.

Table 3-1 The absorbance of 40.0 μg L^{-1} Cu standard working solution at various pyrolysis temperatures

Pyrolysis temperature (°C)	Absorbance ± SD*
1000	0.1506 ± 0.0014
1100	0.1523 ± 0.0029
1200	0.1466 ± 0.0004
1300	0.1435 ± 0.0049
1400	0.1217 ± 0.0032
1500	0.0325 ± 0.0004

* 3 replications, RSD < 4 %

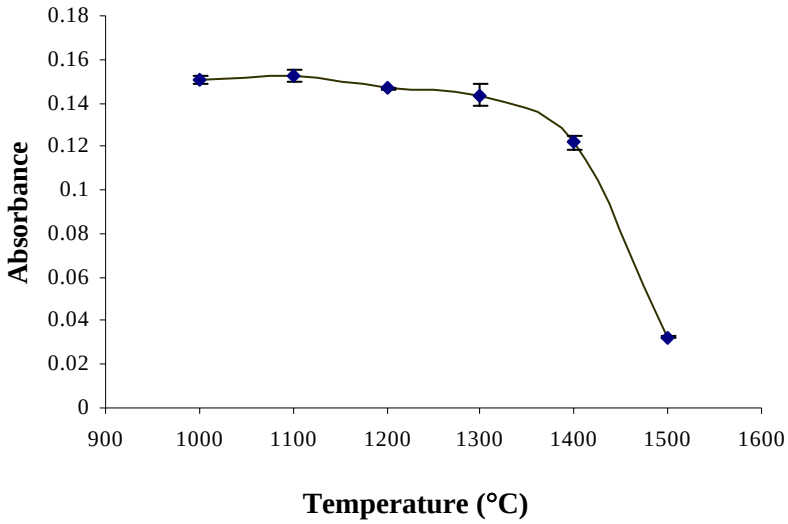

Figure 3-1 The absorbance of 40.0 μg L^{-1} Cu standard working solution at various pyrolysis temperatures

Table 3-2 The absorbance of 4.0 μg L^{-1} Cd standard working solution at various pyrolysis temperatures

Pyrolysis temperature (°C)	Absorbance ± SD*
300	0.2031 ± 0.0019
500	0.1944 ± 0.0035
700	0.1850 ± 0.0024
900	0.1825 ± 0.0027
1000	0.1790 ± 0.0033
1100	0.1237 ± 0.0028

* 3 replications, RSD < 4 %

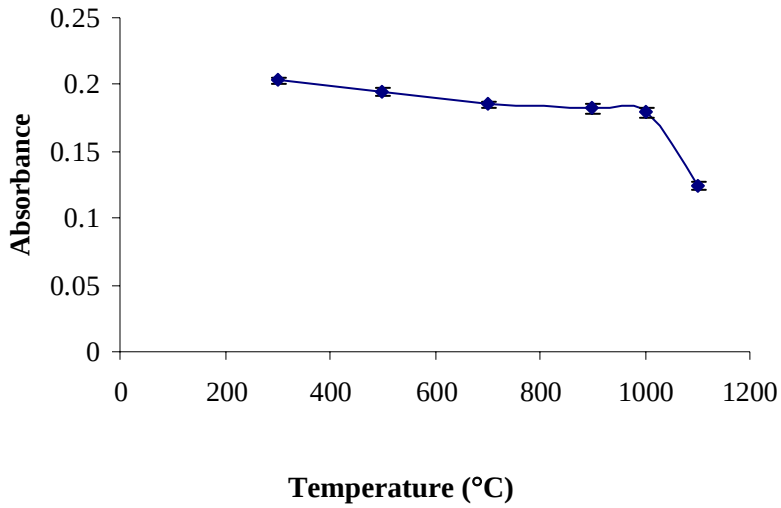

Figure 3-2 The absorbance of 4.0 μg L^{-1} Cd standard working solution at various pyrolysis temperatures

Table 3-3 The absorbance of 80.0 μg L^{-1} Pb standard working solution at various pyrolysis temperatures

Pyrolysis temperature (°C)	Absorbance ± SD*
300	0.1644 ± 0.0034
400	0.1610 ± 0.0047
500	0.1531 ± 0.0036
600	0.1552 ± 0.0043
700	0.1571 ± 0.0039
850	0.1576 ± 0.0048
1000	0.1527 ± 0.0049
1100	0.1528 ± 0.0021
1200	0.1420 ± 0.0028

* 3 replications, RSD < 4 %

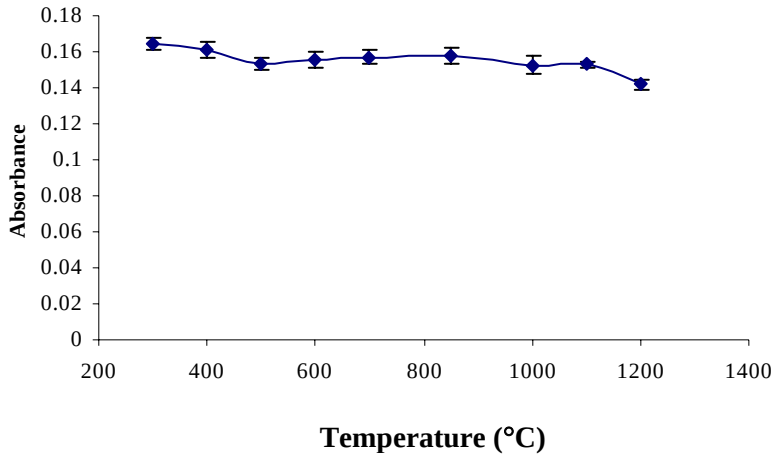

Figure 3-3 The absorbance of 80.0 μg L^{-1} Pb standard working solution at various pyrolysis temperatures

From Table 3-1 to 3-3 and Figure 3-1 to 3-3 the optimum pyrolysis temperature for Cu, Cd and Pb were 1200, 500 and 850 °C, respectively.

3.1.2 Atomization temperature

The purpose of the atomization step is to produce an atomic vapor of the analyte elements, thereby allowing atomic absorption to be measured. The temperature in this step is increased to the point dissociation of volatilized molecular species occurs (Beaty and Kerber, 1993). The atomization temperature should be high enough to complete volatilization of the analyte element. The optimal temperature depends upon the properties of the compound in which the element resides (AAnalyst 800, Perkin-Elmer). The shape of the peak can also indicate whether the atomization temperature should be minimizing peak tailing and keeping integrated time to a reasonable length (Schlemmer and Radziuk, 1999). The results are shown in Table 3-4 to 3-6 and Figure 3-4 to 3-6.

Table 3-4 The absorbance of 40.0 μg L^{-1} Cu standard working solution at various atomization temperatures

Pyrolysis temperature (°C)	Absorbance ± SD*
1700	0.1654 ± 0.0152
1800	0.1589 ± 0.0001
1900	0.1584 ± 0.0028
2000	0.1523 ± 0.0023
2100	0.1423 ± 0.0008
2200	0.1406 ± 0.0014

* 3 replications, RSD < 4 %

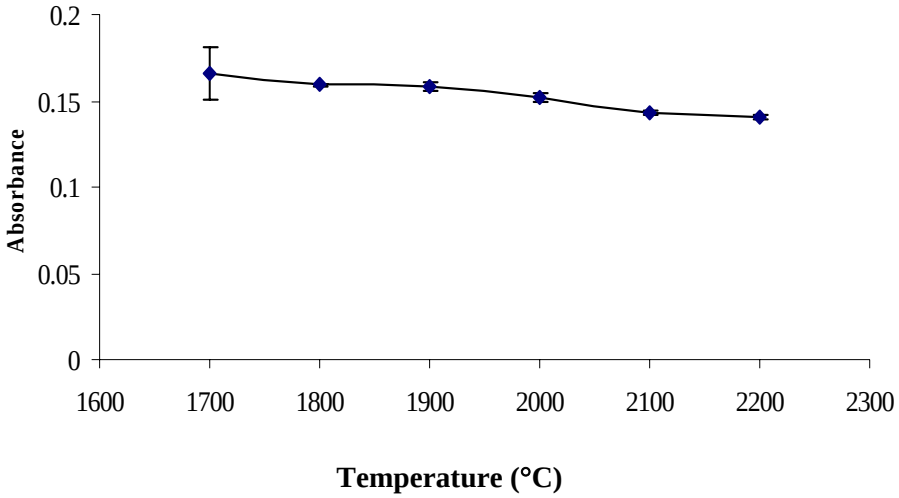

Figure 3-4 The absorbance of 40.0 μg L^{-1} Cu standard working solution at various atomization temperatures

Table 3-5 The absorbance of 4.0 μg L^{-1} Cd standard working solution at various atomization temperatures

Pyrolysis temperature (°C)	Absorbance ± SD*
1300	0.2189 ± 0.0010
1400	0.1976 ± 0.0010
1500	0.1767 ± 0.0059
1600	0.1614 ± 0.0028
1700	0.1525 ± 0.0018
1800	0.1406 ± 0.0024

* 3 replications, RSD < 4 %

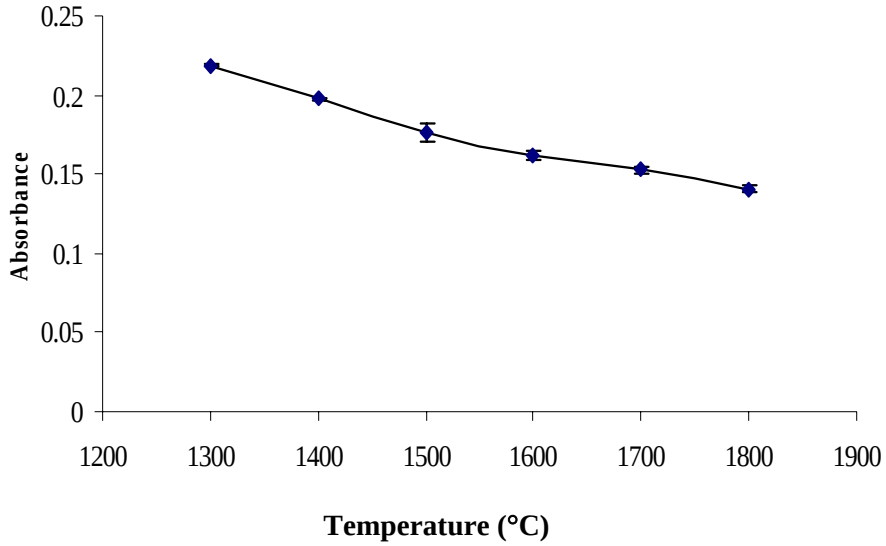

Figure 3-5 The absorbance of 4.0 μg L^{-1} Cd standard working solution at various atomization temperatures

Table 3-6 The absorbance of 80.0 μg L^{-1} Pb standard working solution at various atomization temperatures

Pyrolysis temperature (°C)	Absorbance ± SD*
1300	0.1719 ± 0.0022
1400	0.1725 ± 0.0030
1500	0.1643 ± 0.0015
1600	0.1573 ± 0.0040
1700	0.1454 ± 0.0009
1800	0.1386 ± 0.0013

* 3 replications, RSD < 4 %

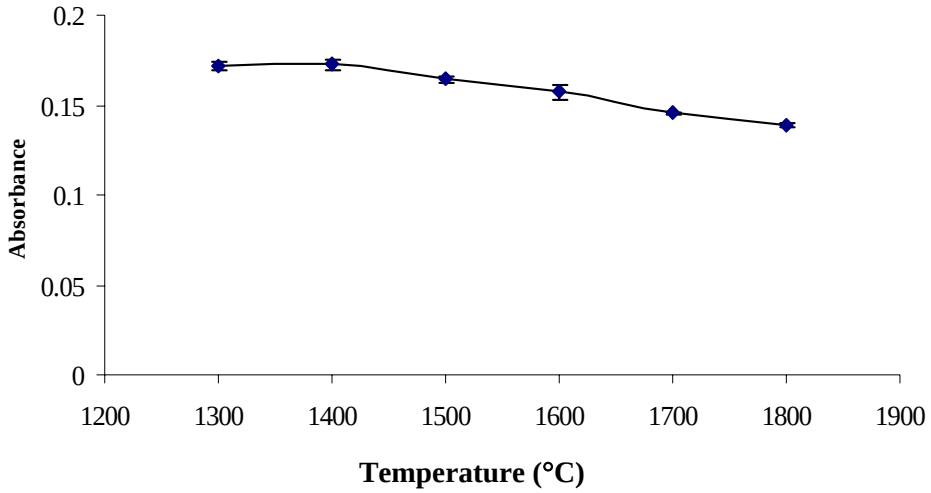

Figure 3-6 The absorbance of 80.0 μg L^{-1} Pb standard working solution at various atomization temperatures

From Table 3-4 to 3-6 and Figure 3-4 to 3-6 the optimum atomization temperature for Cu, Cd and Pb were 2000, 1500 and 1500 ^{o}C, respectively. In addition, Figure 3-7 to 3-9 are shown peak shape of 40.0 μg L^{-1} Cu, 4.0 μg L^{-1} and 80.0 μg L^{-1} Pb standard working solution at optimum temperature.

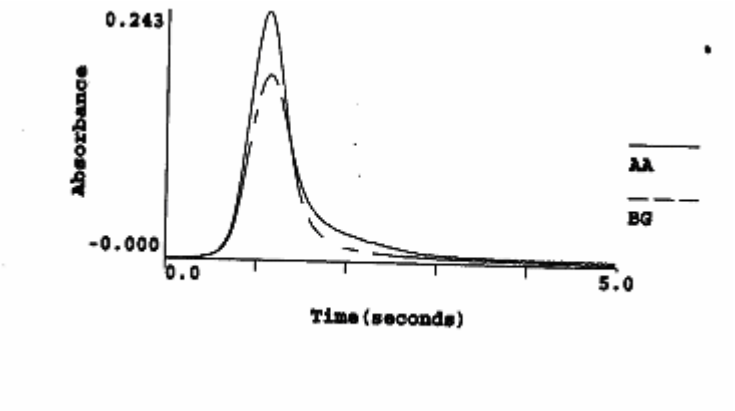

Figure 3-7 Peak shapes of 40.0 μg L^{-1} Cu standard working solution at optimum temperature

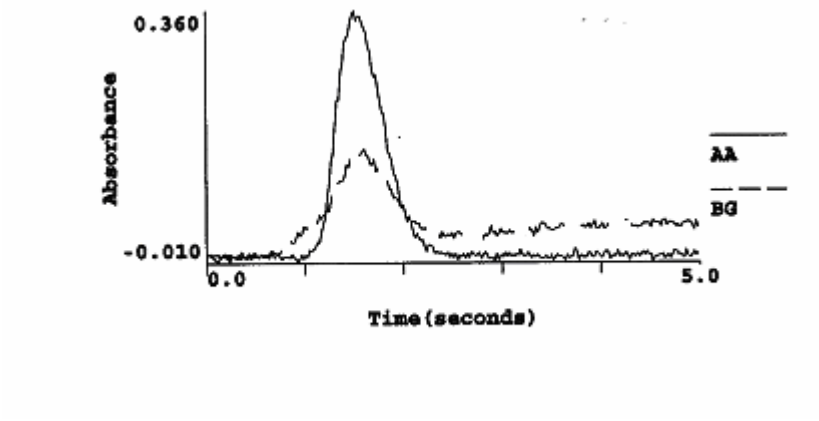

Figure 3-8 Peak shape of 4.0 μg L^{-1} Cd standard working solution at optimum temperature

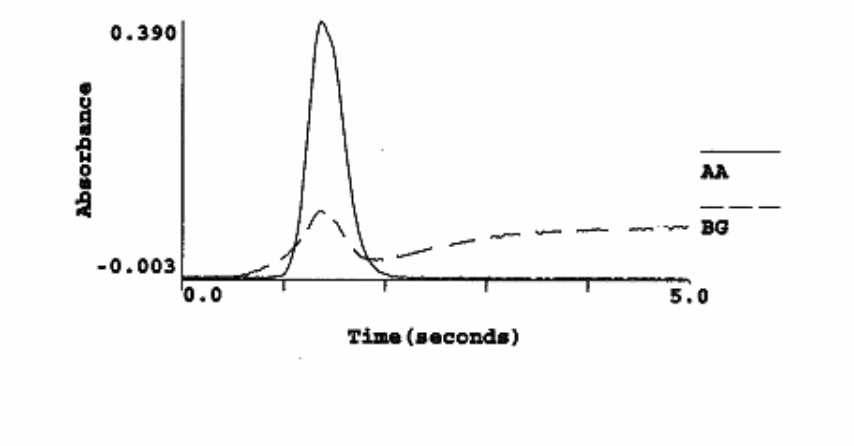

Figure 3-9 Peak shape of 80.0 μg L^{-1} Pb standard working solution at optimum temperature

The optimum conditions for determination of Cu, Cd and Pb by GFAAS are summarized in Table 3-7.

Table 3-7 The optimum conditions of GFAAS for determination of Cu, Cd and Pb

step	Temperature (°C)			Ramp time(s)	Hold time(s)	Internal flow (mL min^{-1})
	Cu	Cd	Pb			
1	110	110	110	1	30	250
2	130	130	130	15	30	250
3	1200	500	850	10	20	250
4	2000	1500	1500	0	5	0
5	2450	2450	2450	1	3	250

3.1.3 The effect of utilizing a matrix modifier and without a matrix modifier for determination of Cu, Cd and Pb

The modifier salt is added to the sample in high concentration to transforming the analyte element into a more well-defined compound. This makes the thermal pyrolysis more predictable and reproducible for a variety of matrices. The use of a matrix modifier that converts the analyte to one common species may eliminate this type of problem with multiple peaks (AAnalyst 800, Perkin-Elmer).

The absorbance of Cu, Cd and Pb standard working solution with utilize modifier from recommended and without modifiers are shown in Table 3-8. Furthermore, peak shape of 40.0 μg L^{-1} Cu, 4.0 μg L^{-1} Cd and 80.0 μg L^{-1} Pb standard working solution with and without modifiers are shown in Figure 3-10 to 3-15.

Table 3-8 The comparison of the absorbance with and without matrix modifier

Element	Type of matrix modifiers	Absorbance	
		With Modifiers (±SD)	Without Modifiers (±SD)
Cu	0.003 mg $Mg(NO_3)_2$+0.005 mg Pd	0.1634 ± 0.0292	0.1619 ± 0.0045
Cd	0.05 mg $NH_4H_2PO_4$+0.003 mg $Mg(NO_3)_2$	0.1944 ± 0.0035	0.1807 ± 0.0050
Pb	0.05 mg $NH_4H_2PO_4$+0.003 mg $Mg(NO_3)_2$	0.1806 ± 0.0015	0.1834 ± 0.0019

* 3 replications, RSD< 4 %

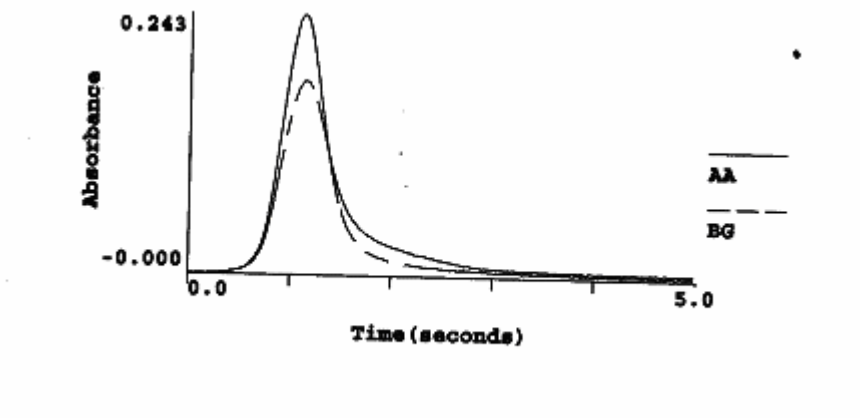

Figure 3-10 Peak shape of 40.0 μg L^{-1} Cu standard working solution with matrix modifiers

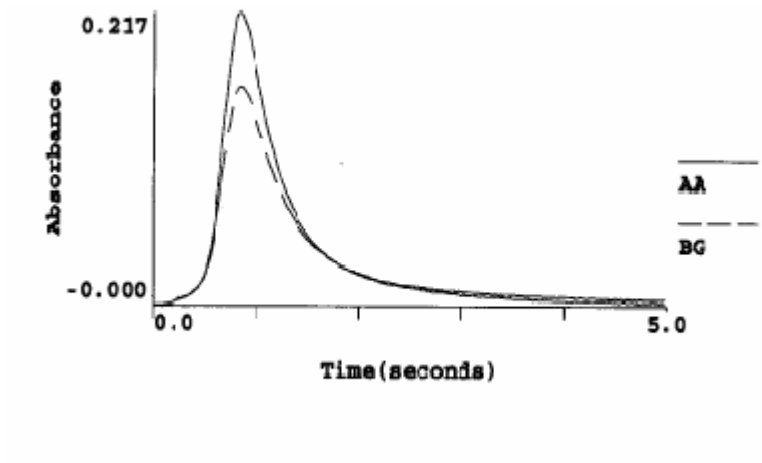

Figure 3-11 Peak shape of 40.0 μg L^{-1} Cu standard working solution without matrix modifiers

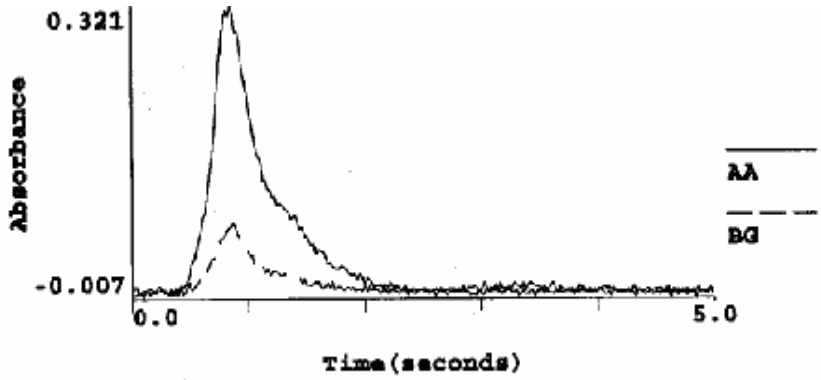

Figure 3-12 Peak shape of 4.0 μg L^{-1} Cd standard working solution with matrix modifiers

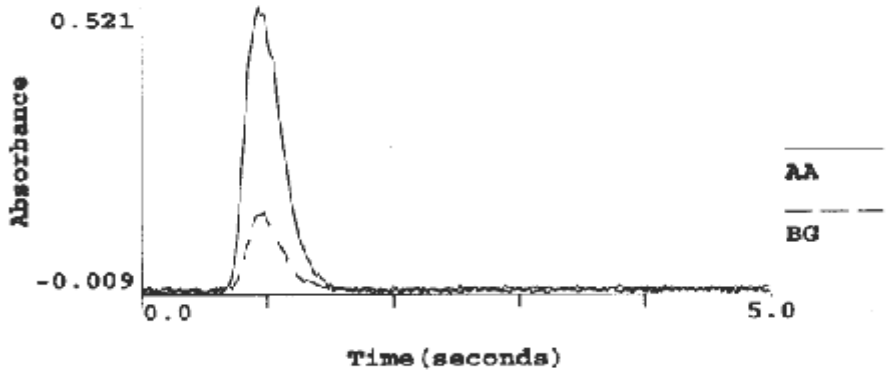

Figure 3-13 Peak shape of 4.0 μg L^{-1} Cd standard working solution without matrix modifiers

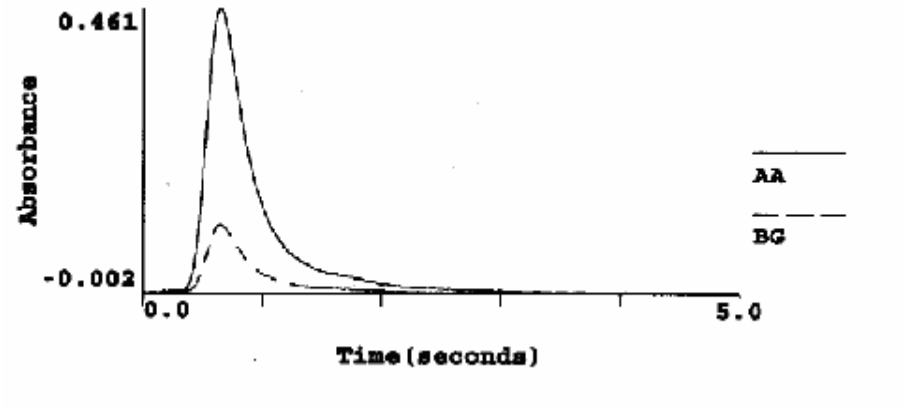

Figure 3-14 Peak shape of 80.0 μg L^{-1} Pb standard working solution with matrix modifiers

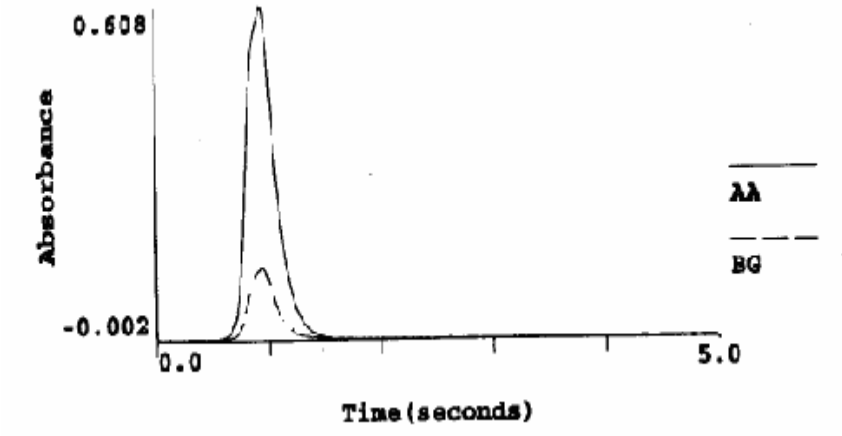

Figure 3-15 Peak shape of 80.0 μg L^{-1} Pb standard working solution without matrix modifiers

From the results, the good peak area and shape obtained when using modifier therefore the matrix modifier was selected for the next experiment.

3.1.4 Type of matrix modifiers

The absorbance of 40.0 μg L^{-1} Cu, 4.0 μg L^{-1} Cd and 80.0 μg L^{-1} Pb standard working solution with various types of matrix modifiers are shown in Table 3-9 to 3-11. In addition, peak shape of 40.0 μg L^{-1} Cu, 4.0 μg L^{-1} Cd and 80.0 μg L^{-1} Pb standard working solution with optimum type of matrix modifier are shown in Figure 3-16 to 3-18.

Table 3-9 The absorbance of 40.0 μg L^{-1} Cu standard working solution at various types of matrix modifiers

Type of matrix modifiers	Absorbance ± SD*
0.005 mg $Mg(NO_3)_2$ + 0.003 mg Pd	0.1644 ± 0.0019
0.005 mg $NH_4H_2PO_4$	0.1584 ± 0.0031
0.003 mg $Mg(NO_3)_2$	0.1636 ± 0.0007
0.005 mg Pd	0.1770 ± 0.0070

* 3 replications, RSD< 4 %

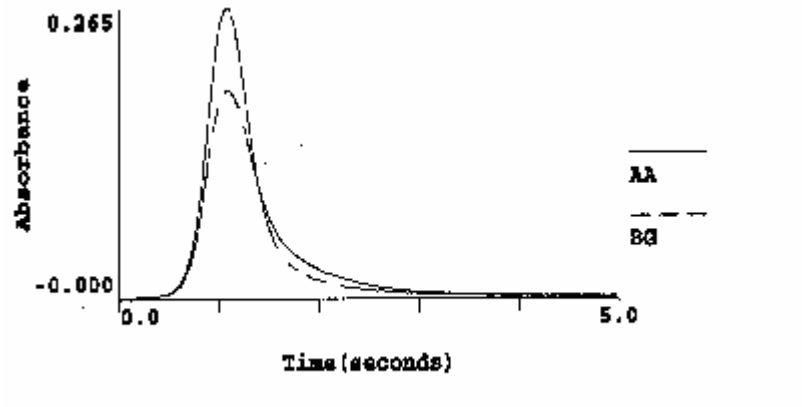

Figure 3-16 Peak shape of 40.0 μg L^{-1} Cu standard working solution at optimum temperature and types of matrix modifiers

Table 3-10 The absorbance of 4.0 μg L^{-1} Cd standard working solution at various types of matrix modifiers

Type of matrix modifiers	Absorbance ±SD*
0.05 mg $NH_4H_2PO_4$+ 0.003 mg $Mg(NO_3)_2$	0.1768 ± 0.0014
0.05 mg $NH_4H_2PO_4$	0.1623 ± 0.0027
0.003 mg $Mg(NO_3)_2$	0.1733 ± 0.0028
0.005 mg Pd	0.1657 ± 0.0029
0.005 mg $La(NO_3)_2$	0.1750 ± 0.2600

* 3 replications, RSD< 4 %

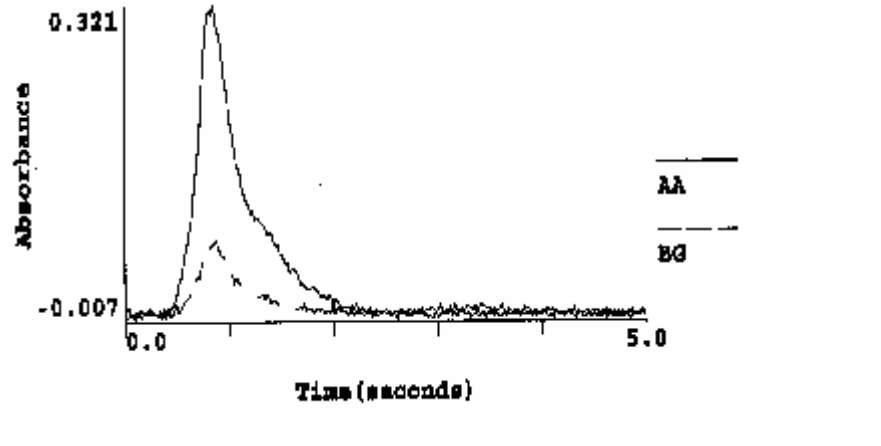

Figure 3-17 Peak shape of 4.0 μg L^{-1} Cd standard working solution at optimum temperature and types of matrix modifier

Table 3-11 The absorbance of 80.0 μg L^{-1} Pb standard working solution at various types of matrix modifiers

Type of matrix modifiers	Absorbance ± SD*
0.05 mg $NH_4H_2PO_4$+ 0.003 mg $Mg(NO_3)_2$	0.1794 ± 0.0014
0.05 mg $NH_4H_2PO_4$	0.1765 ± 0.0037
0.003 mg $Mg(NO_3)_2$	0.1738 ± 0.0024
0.005 mg Pd	0.0488 ± 0.0017
0.005 mg $La(NO_3)_2$	0.1934 ± 0.0015

* 3 replications, RSD< 4 %

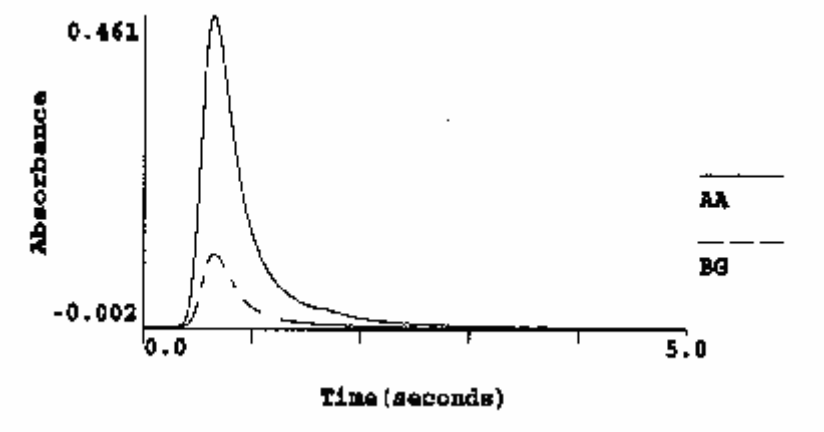

Figure 3-18 Peak shape of 80.0 μg L^{-1} Pb standard working solution at optimum temperature and types of matrix modifier

It was found that the optimum type of matrix modifiers for Cu, Cd and Pb were Pd+$Mg(NO_3)_2$, $La(NO_3)_2$ and $La(NO_3)_2$, respectively.

3.1.5 Linear range

The linear range is determined by plotting the integrated absorbance of the signal versus the concentration of analyte. It is desirable to work within the linear region of the resulting calibration curve (AAnalyst 800, Perkin-Elmer).

Table 3-12 The relation between the peak area and the various Cu standard concentrations (μg L^{-1})

Concentration (μg L^{-1})	Absorbance ± SD*
5.0	0.0041 ± 0.0001
10.0	0.0115 ± 0.0005
25.0	0.0608 ± 0.0006
50.0	0.1478 ± 0.0037
100.0	0.3400 ± 0.0027
150.0	0.5448 ± 0.0048
200.0	0.7293 ± 0.0095

* 3 replications, RSD < 4 %

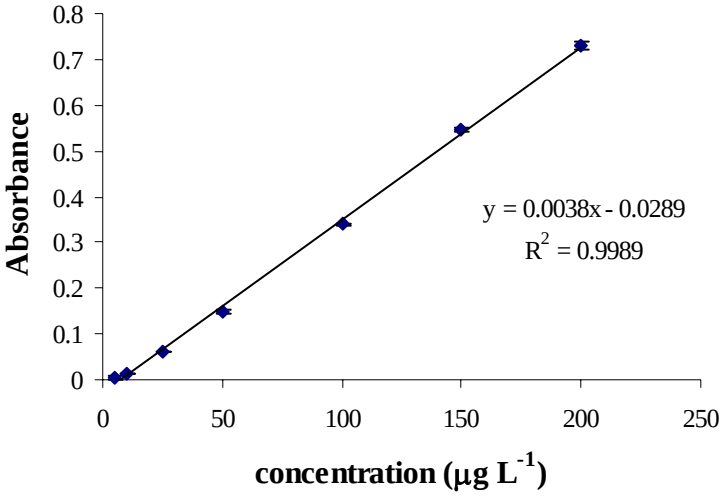

Figure 3-19 The linear dynamic range of Cu standard concentration (µg L^{-1})

Table 3-13 The relation between the peak area and the various Cd standard concentrations (µg L^{-1})

Concentration (µg L^{-1})	Absorbance ± SD*
0.20	0.0110 ± 0.0001
0.40	0.0224 ± 0.0001
1.0	0.0519 ± 0.0015
2.0	0.0987 ± 0.0005
6.0	0.2850 ± 0.0006
8.0	0.3530 ± 0.0001
10.0	0.4313 ± 0.0022

* 2 replications, RSD < 4 %

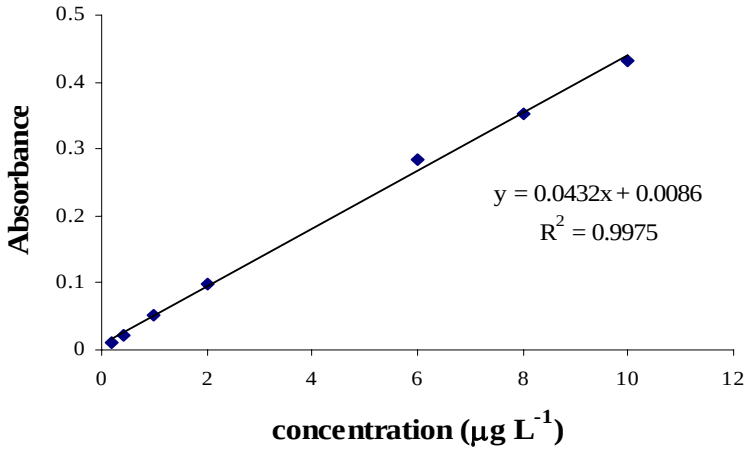

Figure 3-20 The linear dynamic range of Cd standard concentration (µg L^{-1})

Table 3-14 The relation between the peak area and the various Pb standard concentrations (μg L^{-1})

Concentration (μg L^{-1})	Pb ± SD*
5.0	0.0140 ± 0.0002
10.0	0.0276 ± 0.0006
20.0	0.0576 ± 0.0009
40.0	0.1136 ± 0.0001
80.0	0.2172 ± 0.0072
100.0	0.2610 ± 0.0013
120.0	0.3110 ± 0.0010
140.0	0.3514 ± 0.0022
160.0	0.3951 ± 0.0045
200.0	0.4715 ± 0.0045

* 2 replications, RSD < 4 %

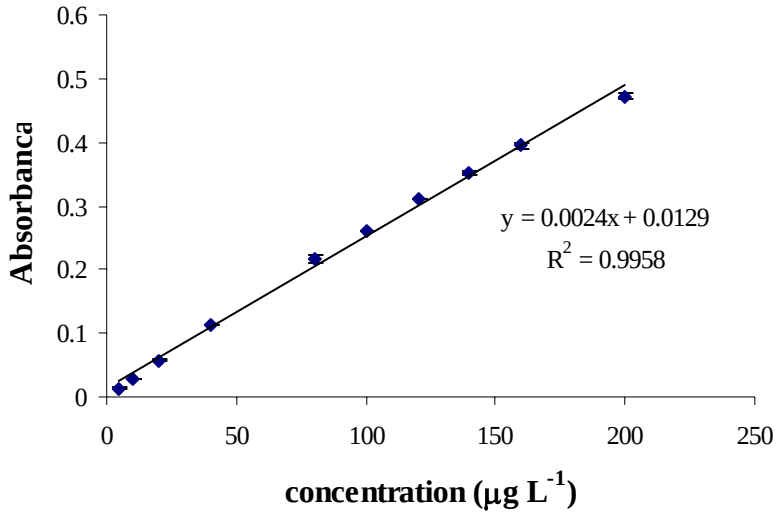

Figure 3-21 The linear dynamic range of Pb standard concentration (μg L^{-1})

The integrated absorbance of Cu, Cd and Pb at various concentrations are shown in Table 3-12 - 3-14 and Figure 3-19 - 3-21. For each concentration, two replications was carried out and obtained high precision for all relative standard deviation (RSD) lower than 4 %. The linear dynamic range of Cu, Cd and Pb were from 5-200, 0.2-10 and 5-200 μg L^{-1}, respectively with a good correlation coefficient, $R^2 > 0.99$.

3.1.6 Detection limit

The detection limit (DL) is defined as the smallest concentration that can be reported as being present in a sample with a specified level of confidence.

Most commonly, the detection limit is defined operationally as the analyte concentration yielding an analytical signal equal to some confidence factor *k* time the SD of the blank measurement (s_{bk}) or the concentration where $S = ks_{bk}$, Alternatively, it can be defined as the analyte concentration where $S/N = k$, which is equivalent to the first definition if $N = s_{bk}$, so $S/N = ks_{bk}/s_{bk} = k$. The DL can also be directly calculated from

$$DL = ks_{bk} / m$$

Here a linear calibration curve near the DL with calibration slope *m* is assumed, so $S = mc$ or $c = S/m$ and $S = ks_{bk}$. The factor *k* is most often chosen to be 2 or 3 (Ingle and Crouch, 1988).

The absorbance of blanks were carried out for evaluating detection limit of Cu, Cd and Pb. The results are shown in Table 3-15 to 3-17 and Figure 3-22 to 3-24. The detection limit of Cu, Cd and Pb are summarized in Table 3-18.

Table 3-15 The data of the blank measurements of Cu, n = 10

Replicate	Absorbance of blank for Cu, n=10
1	0.0000
2	-0.0001
3	-0.0001
4	-0.0004
5	-0.0001
6	-0.0001
7	0.0000
8	0.0001
9	-0.0002
10	-0.0003
	Mean = -0.0001 SD = 0.0001

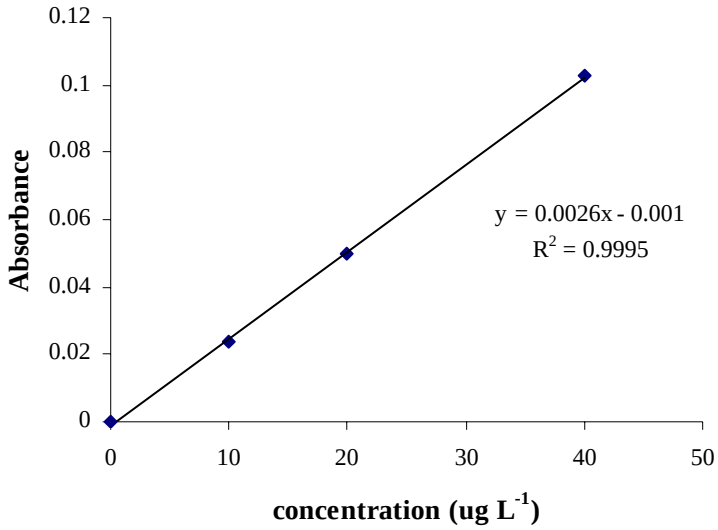

Figure 3-22 The calibration curve of Cu

Table 3-16 The data of the blank measurements of Cd, n = 10

Replicate	Absorbance of blank for Cd, n=10
1	0.0020
2	-0.0047
3	0.0019
4	-0.0018
5	0.0024
6	0.0068
7	-0.0018
8	-0.0003
9	0.0009
10	0.0001
	Mean = 0.0006 SD = 0.0031

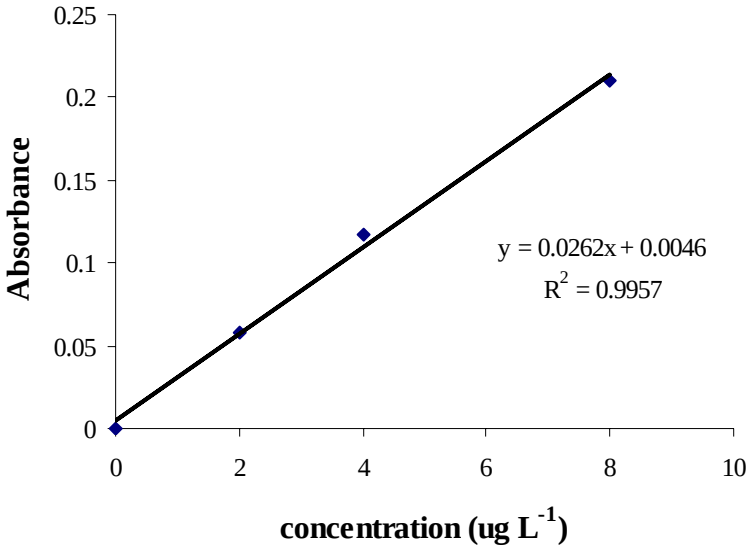

Figure 3-23 The calibration curve of Cd

Table 3-17 The data of the blank measurements of Pb, n = 10

Replicate	Absorbance of blank for Pb, n=10
1	0.0003
2	-0.0006
3	0.0008
4	0.0001
5	-0.0002
6	-0.0007
7	-0.0001
8	0.0002
9	-0.0003
10	0.0002
	Mean = 0.0000 SD = 0.0004

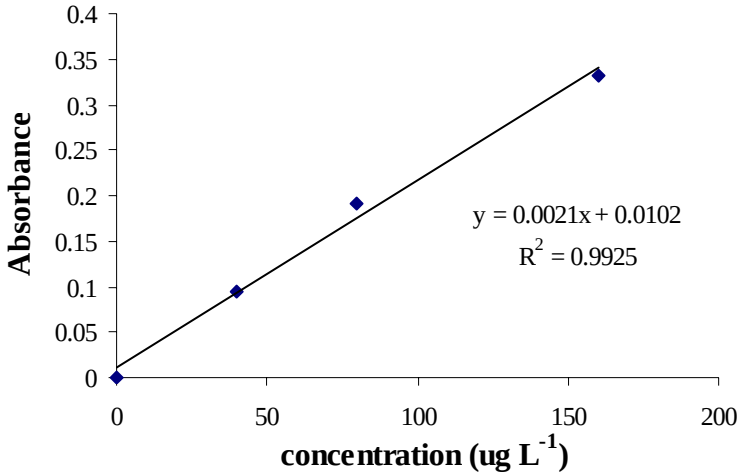

Figure 3-24 The calibration curve of Pb

Table 3-18 The detection limit for Cu, Cd and Pb standard solution with optimum conditions of GFAAS

Parameters	Results		
	Cu	Cd	Pb
Mean	-0.0001	0.0006	0.0000
SD	0.0001	0.0031	0.0004
m	0.0026	0.0262	0.0021
DL = (μg L^{-1})	0.17	0.35	0.64

3.1.7 Accuracy and precision

The accuracy of this technique was evaluated from the percent recovery as mentioned in section 2.3.3.7 and the result is shown in Table 3-19.

Table 3-19 The percent recovery of Cu, Cd and Pb at concentration of 40.00, 8.00 and 80.00 μg L^{-1}, respectively in 1 % (v/v) nitric acid

Metals	Added Amount(μg L^{-1})	Found Amount (μg L^{-1})	% Recovery	%RSD
Cu	40.00	41.10	102.74	2.66
Cd	8.00	8.00	100.02	0.04
Pb	80.0	80.51	100.63	1.09

∗ 3 replications, RSD < 10 %

From this results, it can be concluded that the percentage recovery of Cu, Cd and Pb at 40.00, 8.00 and 80.00 μg L^{-1} were 102.74, 100.02 and 100.63, respectively, in agreement with EPA method 7010 (85-115 %).

In addition, the precision of this method was also evaluated as % RSD. The % RSD of Cu, Cd and Pb was obtained from this method were 2.66, 0.04 and 1.09, respectively, in agree with from EPA method (<10 %).

3.2 Sample preparation using solid phase extraction

3.2.1 Effect of eluent concentration on desorption of Cu, Cd and Pb on Amberlite IRC-748 resin

Desorption of metals is expected to be achieved by proton exchange from acidic solution (Malla *et al*., 2002). The nature of the elution solvent is of prime importance and should optimally meet three criteria: efficiency, selectivity and compatibility. In addition, the elution solvent should be compatible with the analysis technique. In particular, when using both flame and electrothermal AAS, HNO_3 should be preferred to other acids (namely H_2SO_4, HCl), as nitrate ion is a more acceptable matrix (Camel, 2003). Therefore, in this experiment nitric acid using as eluent. The eluent concentrations for preconcentration were varied as in 2.4.2 and the results are shown in Table 3-20 and Figure 3-25.

Table 3-20 Effect of eluent concentration on desorption of Cu, Cd and Pb on Amberlite IRC- 748 resin

Eluent concentration (M)	% Recovery		
	Cu ± SD*	Cd ± SD*	Pb ± SD*
1	55.16 ± 4.24	87.03 ± 7.30	65.36 ± 5.30
3	38.56 ± 0.79	74.36± 4.02	63.71 ± 0.15
5	50.71 ± 0.61	69.89± 2.78	94.03 ± 0.45

* 3 replications, RSD < 10 %

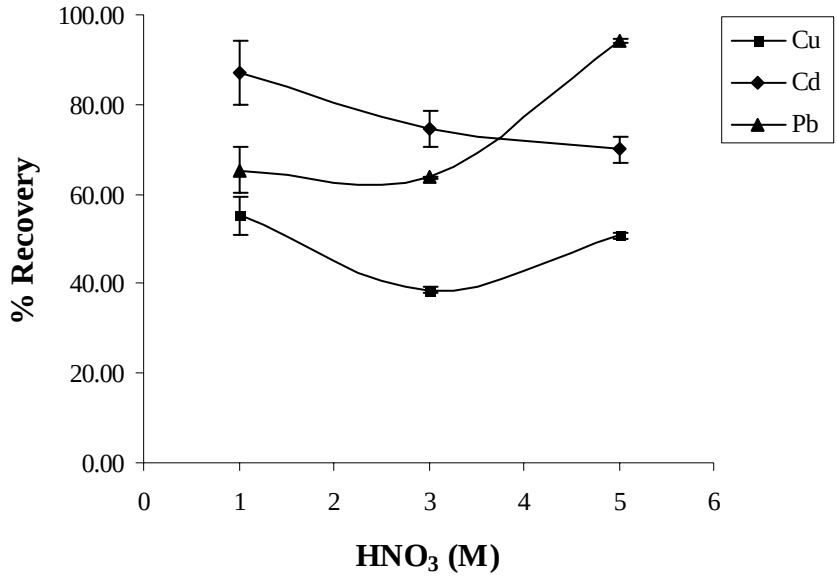

Figure 3-25 Effect of eluent concentration on desorption of Cu, Cd and Pb on Amberlite IRC-748 resin

From the results in Figure 3-25 that the eluent concentration was selected for the elution of the next experiment was 1 M HNO_3 that gives the maximum percentage recovery for Cu and Cd and this concentration was reduced lifetime of graphite tube.

3.2.2 Effect of pH of sample solution on adsorption of Cu, Cd and Pb on Amberlite IRC-748 resin

Sample pH is of prime importance for efficient retention of the trace elements on the sorbent. Its influence strongly depends on the nature of the sorbent used. In particular with ion exchangers, correct adjustment of sample pH is required to ensure preconcentration. Thus, in the case of cationic-exchangers, low pH usually results in poor extraction due to competition between protons cationic species for retention on the sorbent (Camel, 2003). The pH of sample solution was varied as in 2.4.3 and the results are shown in Table 3-21 and Figure 3- 26.

Table 3-21 Effect of pH of sample solution on adsorption of Cu, Cd and Pb on Amberlite IRC-748 resin

pH of sample solution	% Recovery		
	Cu ± SD*	Cd ± SD*	Pb ± SD*
2.5	82.80 ± 5.00	87.45 ± 0.07	95.15 ± 2.18
3.5	80.46± 3.69	96.61 ± 0.05	98.39 ± 1.25
6	55.83± 5.51	97.08 ± 0.33	83.73 ± 6.13
8.5	61.03 ± 3.80	75.74 ± 0.35	62.51 ± 0.42
9.5	47.25 ± 3.93	67.26 ± 0.03	49.92 ± 3.35

* 3 replications, RSD < 10 %

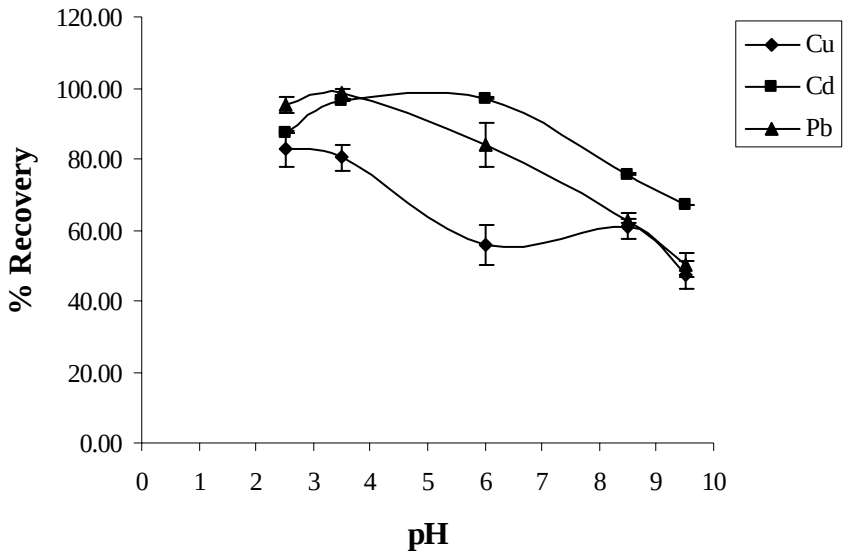

Figure 3-26 Effect of pH of sample solution on adsorption of Cu, Cd and Pb on Amberlite IRC-748 resin

It can be concluded from the results in Figure 3-26 that the solution pH that gives the maximum percentage recovery was 3.5. Consequently, this pH was selected for the preconcentration of the next experiment.

3.2.3 Effect of column volume on adsorption of Cu, Cd and Pb on Amberlite IRC-748

The effect of different column volume on adsorption of Cu, Cd and Pb on Amberlite IRC-748 resin are shown in Table 3-22 and Figure 3-27.

Table 3-22 The percent recovery of Cu, Cd and Pb on Amberlite IRC-748 at different column volume

Volume of resin (mL)	% Recovery		
	Cu ± SD*	Cd ± SD*	Pb ± SD*
0.5	77.42 ± 1.95	99.10 ± 1.70	94.14 ± 0.19
1.0	80.65± 0.93	102.78 ± 2.59	97.64 ± 0.36
1.5	81.24 ± 1.18	99.24 ± 0.67	98.00 ± 1.42
2.0	86.53± 0.59	102.49 ± 1.73	99.62 ± 0.73
2.5	83.89 ± 1.58	99.98± 2.16	100.19 ± 1.90

* 3 replications, RSD< 10 %

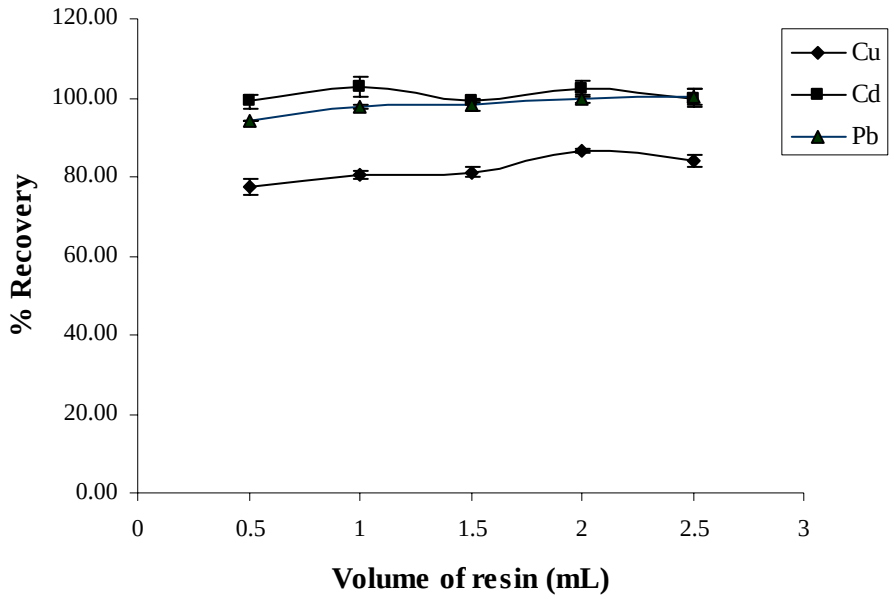

Figure 3-27 The percent recovery of Cu, Cd and Pb on Amberlite IRC-748 at different column volume

It can be concluded from the results in Figure 3-27 that the column volume that gives the maximum percentage recovery was 2.0 mL. Consequently, this volume was selected for preconcentration in the next experiment.

3.2.4 Effect of flow rate on adsorption of Cu, Cd and Pb on Amberlite IRC-748 resin

The flow rate of the solvent should be high enough to avoid excessive duration and low enough to ensure quantitative recovery of the metals. Typically flow rates are in the range of 0.5- 5.0 mL min^{-1} for cartridge (Camel, 2003). The flow rates were varied from 1.0 - 4.0 mL min^{-1} and the results are shown in Table 3-23 and Figure 3-28.

Table 3-23 The percent recovery of Cu, Cd and Pb on Amberlite IRC-748 resin at various flow rates

Flow rate (mL min^{-1})	% Recovery		
	Cu ± SD*	Cd ± SD*	Pb ± SD*
1.0	84.95 ± 7.18	97.88 ± 0.60	103.71 ± 0.95
2.0	86.05 ± 2.68	97.57 ± 0.98	105.99 ± 3.20
4.0	86.86 ± 2.22	98.39 ± 1.54	113.70 ± 8.90

* 3 replications, RSD< 10 %

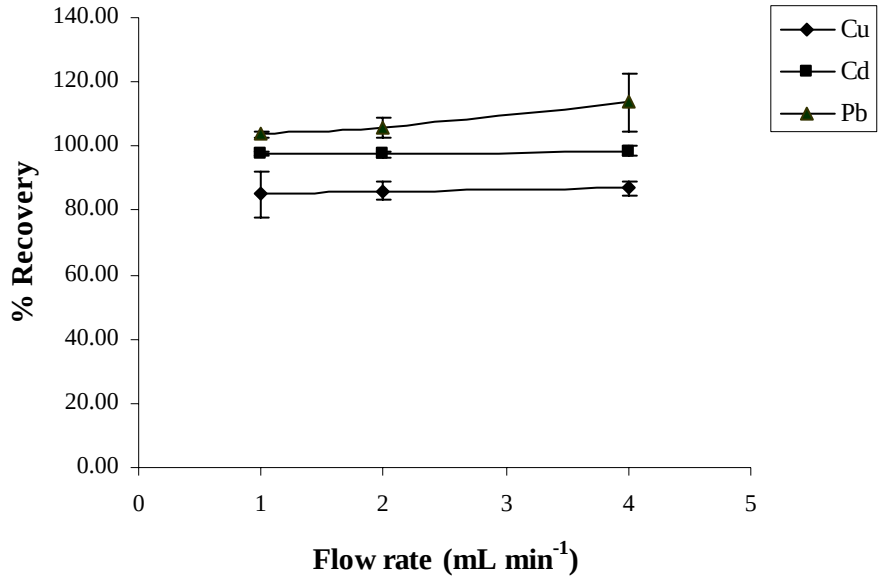

Figure 3-28 The percent recovery of Cu, Cd and Pb on Amberlit IRC-748 resin at various flow rates

From the results obtained in Figure 3-28, it was found that the flow rate 1.0-4.0 mL min^{-1} gave maximum recovery, therefore in order to reduced time for preconcentration this experiment was selected 4.0 mL $min^{-1}$for next experiment.

3.2.5 Effect of eluent volume on desorption of Cu, Cd and Pb on Amberlite IRC- 748 resin

The elution volume may be determined either experimentally or estimated theoretically. Minimum elution volume for a cartridge is typically 120 μL/ 100 mg of the sorbent. The elution volume can usually be reduced by increasing the concentration of the eluting solvent (e.g. acid). The elution step should enable sufficient time and elution volume to permit the metallic species to diffuse out of the solid sorbent pores (Camel, 2003). The volumes of eluents were varied as in 2.4.6 and the results are shown in Table 3-24 and Figure 3-29.

Table 3-24 Effect of eluent volume on desorption of Cu, Cd and Pb on Amberlite IRC-748 resin

Volume of eluent (mL)	% Recovery		
	Cu ± SD*	Cd ± SD*	Pb ± SD*
10.0	63.97 ± 0.55	97.20 ± 1.62	52.26 ± 5.43
25.0	82.29 ± 1.17	94.05 ± 0.16	94.58 ± 1.01
30.0	83.29 ± 3.82	97.33 ± 2.11	96.26 ± 4.51
40.0	86.56 ± 1.66	91.80 ± 0.67	88.62 ± 1.58
50.0	85.58 ± 3.28	93.74 ± 0.44	93.02 ± 1.40

* 3 replications, RSD< 10 %

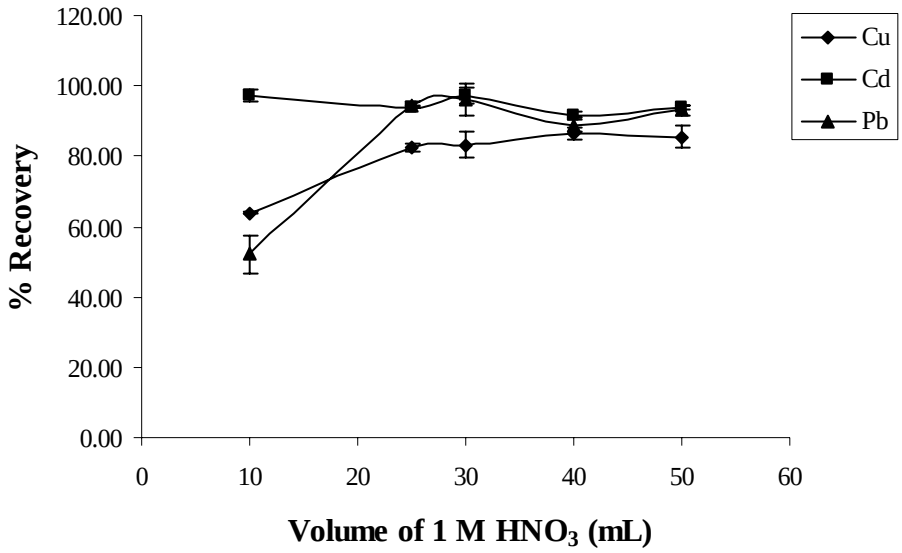

Figure 3-29 Effect of eluent volume on desorption of Cu, Cd and Pb on Amberlite IRC-748 resin

From the results obtained in Figure 3-29 it can be concluded that the optimum eluent volume was 25.0 mL, therefore this eluent volume was selected for the next experiment.

Preconcentration factor for a given volume of the sample solution passed through the column depend upon the original sample volume and the volume of the acid solution required to quantitatively eluting the metal sorpted onto the resin. From Figure 3-29 it was found that 1 M HNO_3, the curve leveled off at an eluted

volume of 25.0 mL. A 250.0 mL of rainwater samples passed through the column therefore an enrichment factor of ten times could be achievable.

3.2.6 The comparison of the calibration and standard addition method for determination of Cu, Cd and Pb in rainwater samples

This experiment was performed to compare standard method between calibration and standard addition for determination of Cu, Cd and Pb in rainwater samples after preconcentration using Amberlite IRC-748 chelating resin. The results are shown in Table 3-25 to 3-27 and Figure 3-30 to 3-32.

Table 3-25 The comparison of peak area using calibration and standard addition method for Cu determination in rainwater

Conc. ($\mu g\ L^{-1}$)	Calibration curve ($\pm$ SD)*	Standard addition ($\pm$ SD)*
0.0	0.0000 ± 0.0009	0.0634 ± 0.0034
20.0	0.0594 ± 0.0029	0.1178 ± 0.0019
40.0	0.1309 ± 0.0068	0.1795 ± 0.0006
80.0	0.2687 ± 0.0032	0.3033 ± 0.0006

* 2 replications, RSD< 10 %

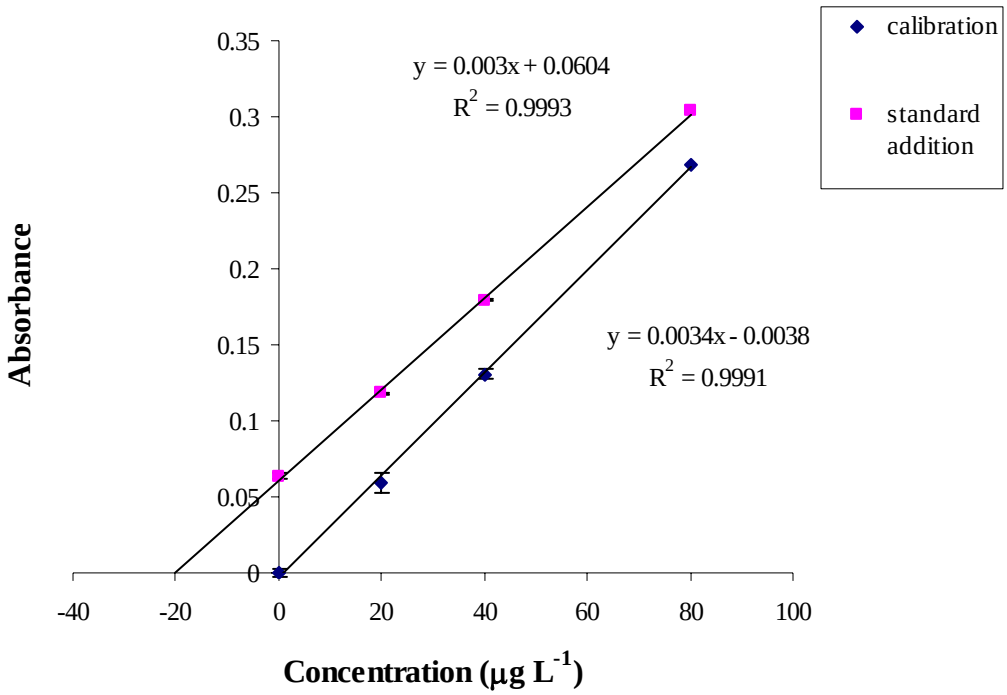

Figure 3-30 The comparison of calibration and standard graph for Cu determination in rainwater

Table 3-26 The comparison of peak area using calibration and standard addition method for Cd determination in rainwater

Conc.(µg L^{-1})	Calibration curve (± SD)*	Standard addition (± SD)*
0.0	0.0000 ± 0.0001	0.0203 ± 0.0008
1.0	0.0569 ± 0.0064	0.0609 ± 0.0005
2.0	0.1144 ± 0.0016	0.1253 ± 0.0015
4.0	0.1991 ± 0.0200	0.2160 ± 0.0008

* 2 replications, RSD< 10 %

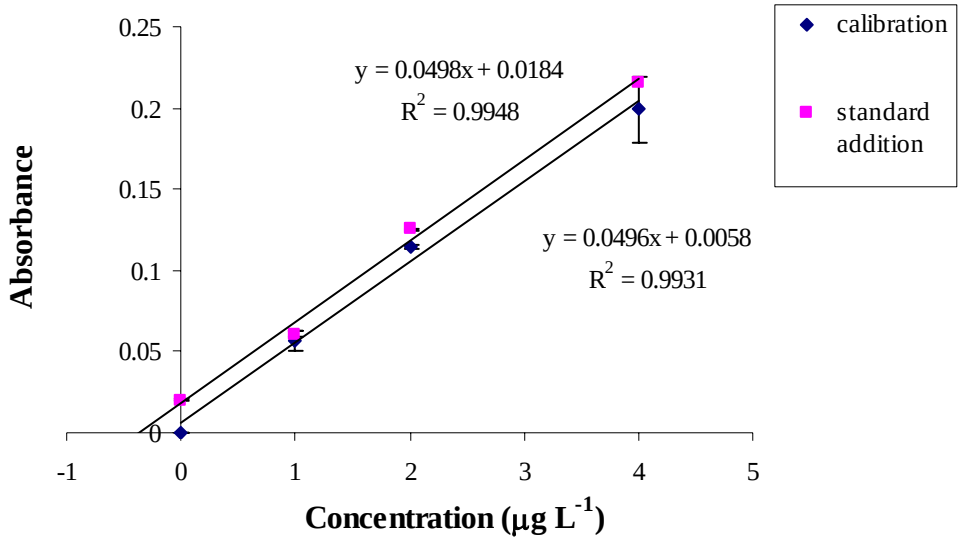

Figure 3-31 The comparison of calibration and standard graph for Cd determination in rainwater

Table 3-27 The comparison of peak area using calibration and standard addition method for Pb determination in rainwater

Conc. (μg L^{-1})	Calibration curve (± SD)*	Standard addition (± SD)*
0.0	0.0000 ± 0.0004	0.0374 ± 0.0005
20.0	0.0506 ± 0.0004	0.0814 ± 0.0001
40.0	0.1066 ± 0.0023	0.1263 ± 0.0005
80.0	0.2038 ± 0.0036	0.2083 ± 0.0008

* 2 replications, RSD< 10 %

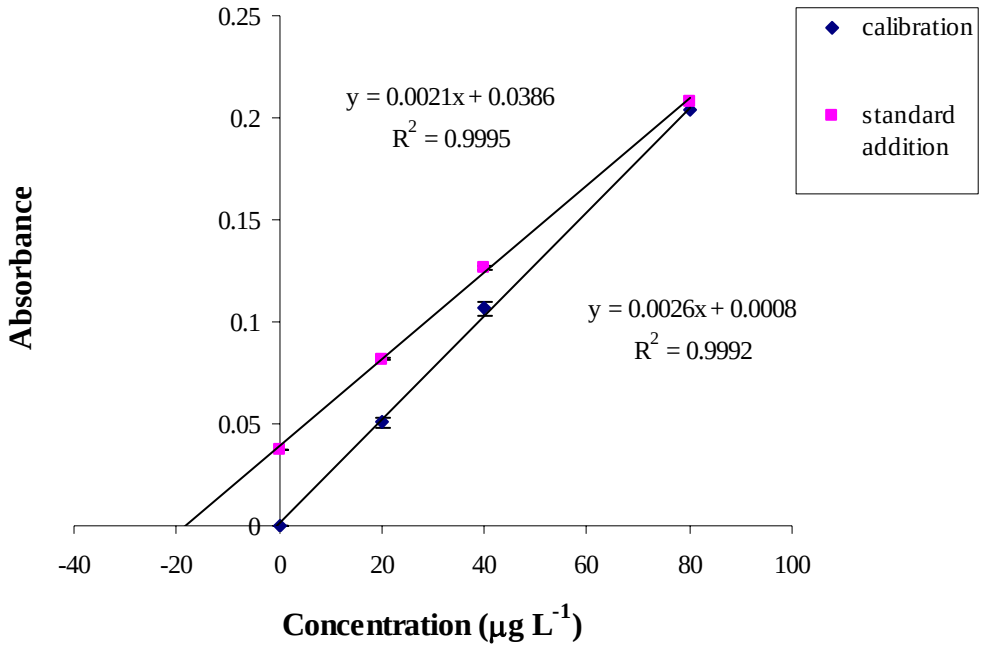

Figure 3-32 The comparison of calibration and standard graph for Pb determination in rainwater

From Table 3-25 to 3-27 and Figure 3-30 to 3-32, it was found that the slope of Cu and Pb when compare with calibration and standard addition method do not parallel where different with Cd. It can be concluded that there is a matrix interference occur in rainwater sample. Therefore, in this experiment was selected a calibration method for Cd and standard addition method for of Cu and Pb determination in rainwater samples.

3.2.7 The study of percentage recovery of Cu, Cd and Pb in rainwater, drinking water and deionized water

The analytical recovery of Cu, Cd and Pb added to water samples are shown in Table 3-28

Table 3-28 Analytical recovery of Cu, Cd and Pb added to some water samples

Water sample type	Concentration of metals added ($\mu g\ L^{-1}$)	% Recovery (±SD)*		
		Cu	Cd	Pb
Rainwater	1.0	101.77 ± 4.89	112.28 ± 1.75	54.35 ± 3.89
	5.0	-	111.76 ± 1.43	-
	10.0	105.56 ± 2.62	-	101.80 ± 9.81
Drinking water	1.0	55.05 ± 8.56	92.56 ± 4.54	113.17 ± 84.75
	5.0	-	101.07 ± 1.44	-
	10.0	70.88 ± 6.41	-	76.35 ± 11.03
Deionized water	1.0	93.65 ± 8.84	105.01 ± 2.73	99.70 ± 3.54
	5.0	-	103.04 ± 1.95	-
	10.0	113.86 ± 6.98	-	128.92 ± 9.62

* 3 replications, RSD< 10 %

In order to establish the validity of this procedure the method has been applied to determine Cu, Cd and Pb in rainwater, drinking water and deionized water samples. The result is shown in Table 3-28. The percentage recovery of Cu, Cd and Pb at 10.0, 5.0 and 10.0 $\mu g\ L^{-1}$ in rainwater, drinking water and deionized water samples were 70.88-128.92 $\mu g\ L^{-1}$. From this result it was found that this method is suitable for preconcentration of Cu, Cd and Pb in rainwater samples prior to determine by GFAAS.

3.2.8 Accuracy and precision

The accuracy of SPE-GFAAS was evaluated from the percent recovery as mention in section 2.4.8 and the result is shown in Table 3-28.

From this results, it can be concluded that the percentage recovery of Cu, Cd and Pb at 10, 5 and 10 $\mu g\ L^{-1}$ were 105.6, 111.8 and 101.8 %, respectively.

In addition, the precision of this method was also as %RSD. The %RSD of Cu, Cd and Pb was obtained from this method were 2.48, 1.28 and 9.64, respectively.

3.2.9 Determination of Cu, Cd and Pb in rainwater samples

Nine samples of rainwater were collected in Hat Yai City Municipality (2.5.1). Rainwater samples were preconcentrated by Amberlite IRC-748 resin and analyzed by GFAAS at optimum conditions. The results are shown in Table 3-29 to 3-31 and Figure 3-33 to 3-45.

Table 3-29 The concentration of Cu in nine rainwater samples

Locations	Concentrations ($\mu g\ L^{-1} \pm SD^{*}$)
1. Department of Chemistry, Prince of Songkla University	0.79 ± 0.56
2. Kuanlung Cross-road	0.18 ± 0.01
3. Jiranakorn Stadium	1.39 ± 0.16
4. Fountain Circus	1.24 ± 0.23
5. Srinakorn School	0.39 ± 0.05
6. Hat Yai Municipal Park	0.71 ± 0.01
7. Hat Yai Railway Station	0.76 ± 0.09
8. Hat Yai Wittayalai Somboonkulkanya School	0.15 ± 0.02
9. Makro Supermarket	1.05 ± 0.19

* 3 replications

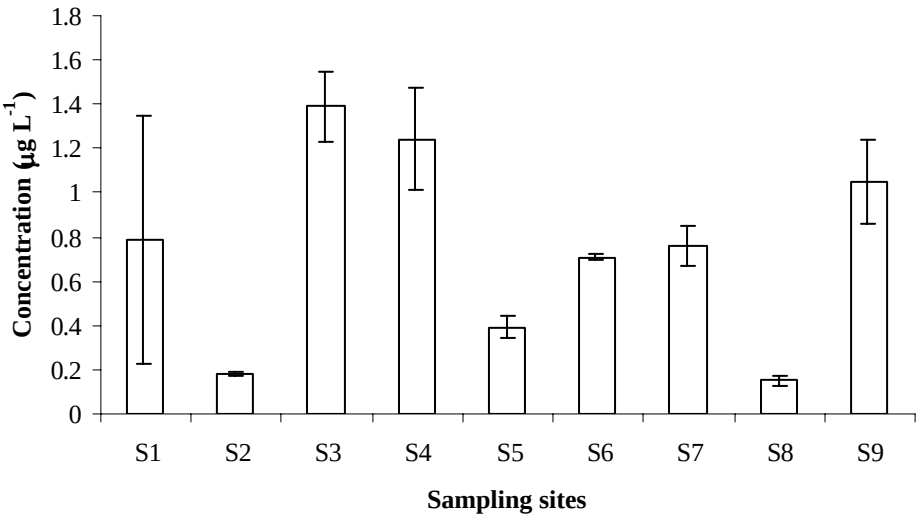

Figure 3-33 The concentration of Cu in nine rainwater samples (preconcentration factor = 10) S1 = Prince of Songkla University, S2 =Kuanlung Cross-road, S3= Jiranakorn Stadium, S4= Fountain Circus, S5=Srinakorn School, S6=Municipal Park, S7= Railway Station, S8=Hat Yai Wittayalai Somboonkulkanya School, S9=Makro Supermarket

Table 3-30 The concentration of Cd in nine rainwater samples

Locations	Concentrations ($\mu g\ L^{-1} \pm SD^{*}$)
1. Department of Chemistry, Prince of Songkla University	0.11 ± 0.001
2. Kuanlung Cross-road	0.08 ± 0.001
3. Jiranakorn Stadium	0.22 ± 0.01
4. Fountain Circus	0.07 ± 0.002
5. Srinakorn School	0.07 ± 0.005
6. Hat Yai Municipal Park	0.44 ± 0.05
7. Hat Yai Railway Station	0.28 ± 0.12
8. Hat Yai Wittayalai Somboonkulkanya School	0.06 ± 0.01
9. Makro Supermarket	1.86 ± 0.01

* 3 replications

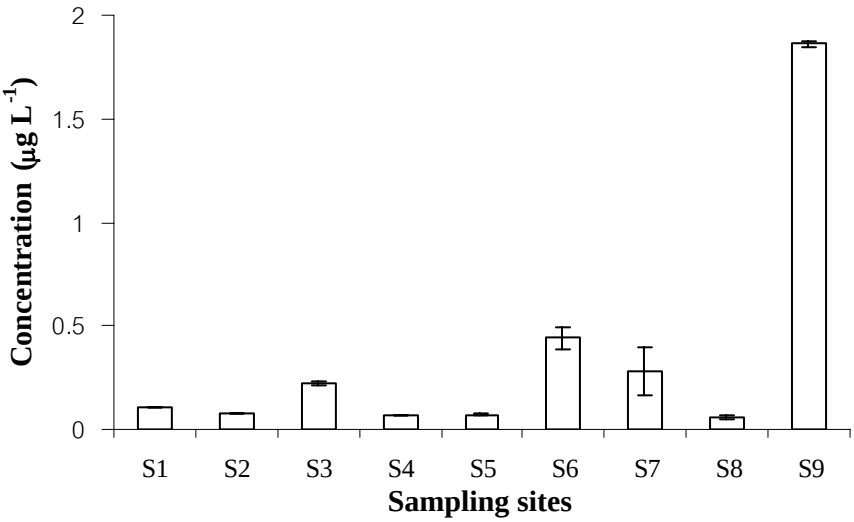

Figure 3-34 The concentration of Cd in nine rainwater samples (preconcentration factor = 10) S1 = Prince of Songkla University, S2 =Kuanlung Cross-road, S3= Jiranakorn Stadium, S4= Fountain Circus, S5=Srinakorn School, S6=Municipal Park, S7= Railway Station, S8=Hat Yai Wittayalai Somboonkulkanya School, S9=Makro Supermarket

Table 3-31 The concentration of Pb in nine rainwater samples

Locations	Concentrations ($\mu g\ L^{-1} \pm SD^{*}$)
1. Department of Chemistry, Prince of Songkla University	1.20 ± 0.25
2. Kuanlung Cross-road	1.13 ± 0.07
3. Jiranakorn Stadium	5.74 ± 1.89
4. Fountain Circus	0.83 ± 0.12
5. Srinakorn School	0.52 ± 0.07
6. Hat Yai Municipal Park	6.85 ± 0.05
7. Hat Yai Railway Station	7.57 ± 1.33
8. Hat Yai Wittayalai Somboonkulkanya School	1.64 ± 0.11
9. Makro Supermarket	34.51 ± 1.53

* 3 replications

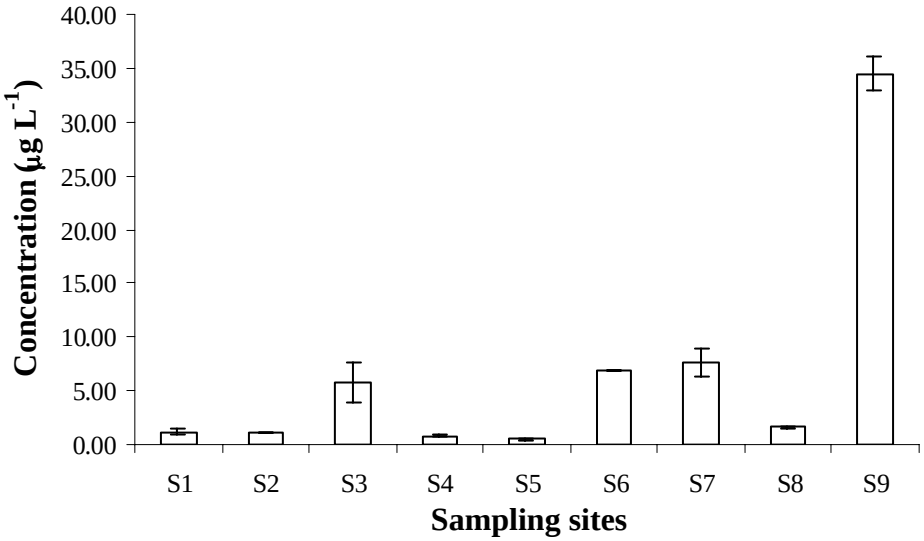

Figure 3-35 The concentration of Pb in nine rainwater samples preconcentration factor = 10) S1 = Prince of Songkla University, S2 =Kuanlung Cross-road, S3= Jiranakorn Stadium, S4= Fountain Circus, S5=Srinakorn School, S6=Municipal Park, S7= Railway Station, S8=Hat Yai Wittayalai Somboonkulkanya School, S9=Makro Supermarket

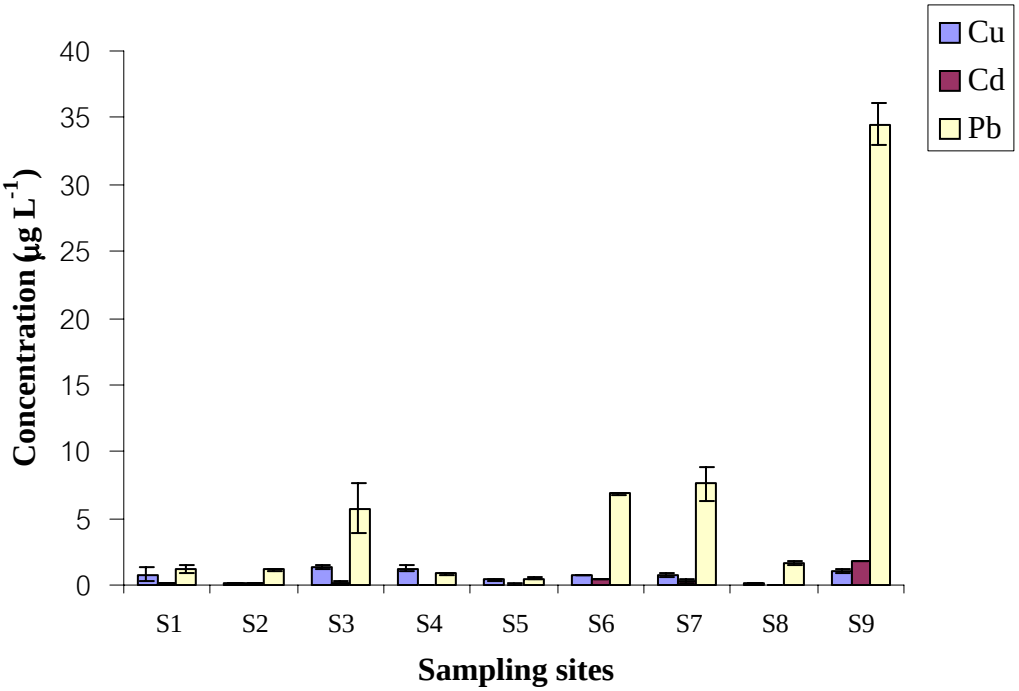

Figure 3-36 The concentration of Cu, Cd and Pb in nine rainwater samples (preconcentration factor = 10, n=3) S1 = Prince of Songkla University, S2 =Kuanlung Cross-road, S3= Jiranakorn Stadium, S4= Fountain Circus, S5=Srinakorn School, S6=Municipal Park, S7= Railway Station, S8=Hat Yai Wittayalai Somboonkulkanya School, S9=Makro Supermarket

Nine rainwater samples were collected during 15/10/2004-11/12/2004. These periods, there was northeast storm. The pH of nine rainwater samples is in the range from 3.85-6.06. The most pH of rainwater samples lower than 5.5 is indicated as acid rainwater.

The results shown that concentration of dissolved form of Cu, Cd and Pb in nine rainwater samples (preconcentration factor = 10) in the range from 0.15-1.39, 0.06-1.86 and 0.52-34.51 µg L^{-1}, respectively. The orders of heavy metals concentration are as follow: Pb > Cd > Cu. However, from the work of Struck *et al.*, 1996 it was found that the concentration of Pb in rainwater samples could found large amount of Pb adsorbed on solid particles and Cd it was found large amount in dissolved in rainwater dominates.